International Journal of Nanoelectronics and Materials
*Volume 16 (Special Issue) December 2023* [195-205]

# Investigation on Sensitivity Amplification Factor of DGFET Electrochemical Sensors for pH Detection

Hanim Hussin[1,4,*], Yasmin Abdul Wahab[2], Norhayati Soin[3,4], and Maizan Muhamad[1]

[1]School of Electrical Engineering, College of Engineering, Universiti Teknologi MARA, 40450 Shah Alam, Selangor
[2]Nanotechnology & Catalysis Research Centre, University of Malaya, Kuala Lumpur
[3]Department of Electrical Engineering, Faculty of Engineering, University of Malaya, Kuala Lumpur
[4]Center of Printable Electronics, Research Management Center, University of Malaya, Kuala Lumpur

**ABSTRACT**

*There has been an increasing interest in the development of chemical and biological FET-based sensors due to their remarkable benefits in label-free detection that has been commonly used in both pH and DNA sensing respectively. In this work, recent Double-Gated Field Effect Transistor (DGFET) as transducers is investigated to understand the super-Nernstian response by amplifying the sensitivity capability in back-gate operations. The BioSensorLab tool was employed to evaluate pH-sensitivity amplification by studying the electrolyte screening and conduction modulation mechanisms which modeled by using Poisson-Boltzmann and Drift-Diffusion equations. The pH sensitivity amplification factors were investigated based on different geometrical configurations of DGFET devices, biasing conditions, and top oxide-electrolyte interfaces. pH sensitivity beyond Nernst limit was observed and increased linearly with the back oxide thickness of the DGFETs. DGFET with a sensitivity of 32.1 mV/pH operated through front-gate operation can be amplified to 195.4 mv/pH through the back-gate operation with a drain voltage of 0.5 V when the back gate oxide thickness increased to 150 nm. Higher pH-sensitivity responses of more than 200 mV/pH were observed where $Al_2O_3$ and $Ta_2O_5$ are used for the top oxide-electrolyte. It can be concluded that pH sensing of back gate operation ensures the DGFET transducers operated beyond the Nernst limit.*

**Keywords:** Sensors, pH detection, Double Gate Field Effect Transistor; dielectric

## 1. INTRODUCTION

Field effect devices as transducer for pH sensing have been employed in a broad applications, such as in healthcare, food safety as well as in environmental monitoring [1][2][3]. The ion-sensitive field-effect transistor (ISFET) sensor first introduced in 1970 by Piet Bergveld is based on potentiometric techniques that has been extensively examined as a transducer due to its potential for label-free detection, fast response, miniaturization, easy integration, parallel sensing, low cost and easy for integration with complementary metal-oxide semiconductor (CMOS) processing technologies [4][5][6][7]. Hence, the measurement of ionic content or pH of an analyte for single molecular detection and point-of-care diagnostics based on FET-based sensor is critical in wide range of applications [8].

In principle, the pH sensitivity of a single gate FET-based sensor can accomplish best pH sensitivity, 59 mV/pH as stated by the Nernstian response [9][10]. In reality however, the theoretical response limit is lowered due to the effects of semiconductor capacitance and electrolyte screening [11]. The performance of single ISFET sensors can be improved by using double gated field effect transistors (DGFETs) structure by amplifying the signal caused by the pH change [12][13].

* Corresponding authors: hanimh@uitm.edu.my

Many research conducted to further improve the limitation of FET-based sensors included type of channel materials, dielectric materials as well as different configurations of the FET, and biasing conditions [9], [11], [14]–[18]. The relation between the geometrical variation based on the scaled size of the transistor channel consists of the length and width, different top and bottom oxide thickness as well as the types of dielectrics used with the amplification effects were not clearly seen based on these approaches.

This paper presents a comprehensive simulation study on the effect of geometric variations, biasing conditions, and gate oxide materials of Double Gate Field Effect Transistors (DGFET) as transducers for pH detection. The sensitivity performance was investigated based FET channel size which include the length and width, top and bottom oxide thicknesses. The sensitivity performance was also investigated based on the conventional Silicon dioxide ($SiO_2$) and compared with high-k dielectrics such as the Aluminum oxide ($Al_2O_3$) and Tantalum pentoxide ($Ta_2O_5$). We investigated how the pH sensor responded during different biasing conditions namely front gate and back gate biased. Critical insights associated to the sensitivity respond determined from $SiO_2$, $Al_2O_3$ and $Ta_2O_5$ in the development of DGFET transducers for sensitivity amplification is also highlighted. We showed that the back gate operation enhances the sensitivity thus able to beat the Nernst limit.

### 1.1 Basic Operation Principle of Field Effect Devices as Transducers for pH Detection

Potentiometric techniques allow the detection of hydrogen ions (H+ or H-) that measured by the changes of surface potential (ψ0) in the dielectric-electrolyte interface [4]. Based on the pH value of the electrolyte, protonation/de-protonation on the gate insulator by the OH groups led to the change in the dielectric surface charge. The protonation of the solution is because lower pH value will generate positive surface charges while higher pH value will generate negative surface charges. The value of surface potential is determined by the resultant charge and biasing conditions. Biasing conditions involve the electrolyte voltage applied through the fluid/front gate voltage or known as reference electrode, as well as the drain bias. Therefore, the basic operation principle of pH sensor relied on the certain gate and drain bias of the transistor as transducer, change in pH that led to the surface charge variation in the oxide-electrolyte interface hence the conductance of the channel material will be altered. The Gouy-Chapman-Stern (GCS) model together with site-binding (SB) theory was able to explain the connection between the pH of the solution and transistor's surface potential [14][12]. The sensitivity can be calculated as

$$\frac{d\psi_0}{dpH} = 2.303\alpha\frac{kT}{q} \tag{1}$$

$\psi_0$ : Surface potential at the oxide-electrolyte interface
$\alpha$ : Dimensionless sensitivity parameter that depends on the intrinsic buffer capacitance of gate dielectric and the ionic concentration of buffer solution
k : Boltzmann's constant
T : Absolute temperature
q : Elementary charge

The gate dielectric of conventional ISFET showed highest pH sensitivity stated as Nernst limit (59.2 mV/pH) which can be obtained when the temperature is 300K, and sensitivity parameter, α at approximately unity. The pH sensitivity is always lower than this limit for a single gate operation and can be enhanced for Super Nernst effects using double gated field effect transistors (DGFET)[1], [9] and extended gated field effect transistors (EGFET)[19]. Figure 1 (a), (b) and (c) shows the conventional ISFET, DGFET and EGFET respectively.

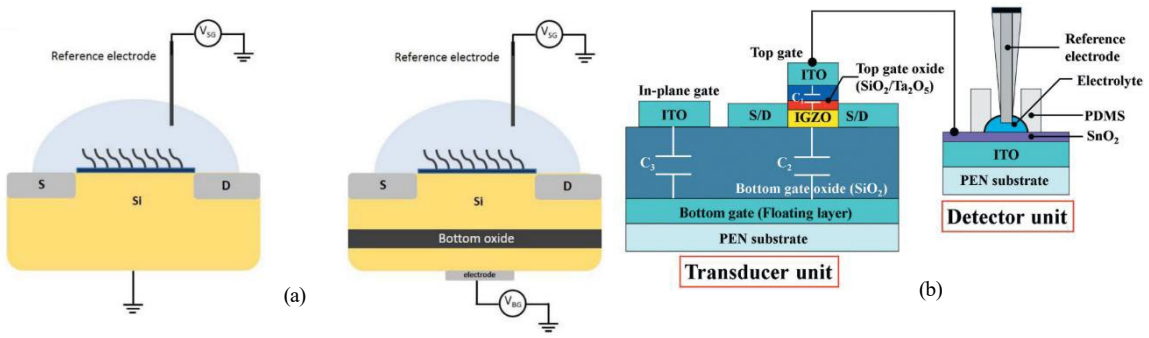


**Figure 1.** The different configuration of ISFET-based sensors (a) Conventional ISFET and (b) Double-gated ISFET [2] (c) Extended gated ISFET [19]. Reprinted from reference [2] and [17], under the terms of the Creative Commons CC BY license.

## 2. METHODOLOGY

Implementation of this work was based on a numerical simulation using BioSensorLab [20]. In this work, well-founded models from previous published research were used within the self-consistent theoretical framework calculated using BiosensorLab to investigate the effects of varying geometrical parameters and applied bias conditions on pH sensitivity. The schematic of the biosensor transistor under study and its one-dimensional schematic used in this work is as shown in Figure 2. The nanoscale FET structure consists of an electrolyte solution comprising target biomolecules. Biomolecules carry significant charges, and this FET-based sensor can be used to detect them. This transducer is able to sense charged biomolecules identical the DNA/protein if detected by the correct receptors or the pH of the electrolyte based on protonation or deprotonation reactions. Based on Figure 2 (b), the underlying model formalism used in BioSensorLab is divided into four regions with detailed explanation on equations used in [11]. Region (I) is the fluid gate-electrolyte interface, region (II) is the electrolyte, region (III) is the top oxide-electrolyte and region (IV) is the oxide-Si FET system. The front or top oxide is above the Si body, while the back oxide is below the Si body.

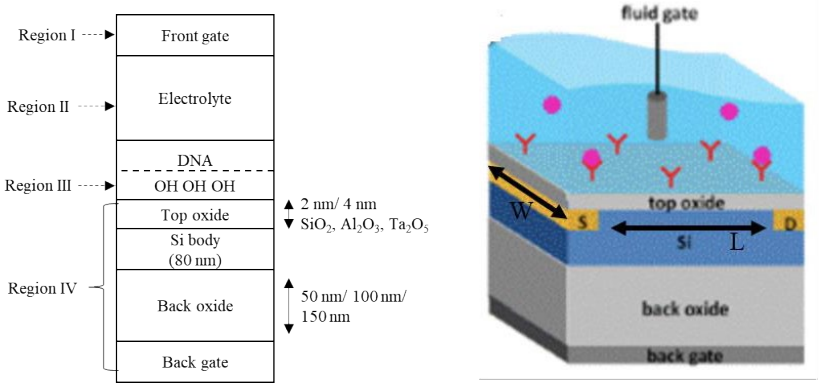


**Figure 2.** (a)1D schematic of DGFET biosensor showing structure based on region with simulated thickness ranges of top and bottom oxide thickness and types of top oxide used. (b) 2D simulated structure [20].

General formulation involves electrostatics in various regions in the system. It is assumed that the ions in bulk electrolyte behave based on the Boltzmann distribution. Overall potential within the electrolyte system is calculated using the Poisson equation. For this simulation, the sensor is basically the double gate field effect device where the region between electrolyte and the top gate

oxide interface was activated with capture probe (receptor) molecules, with surface groups (-OH). For top oxide region, the surface binding model is used to calculate the net charge of OH groups [9], [15]. Protonation and deprotonation mechanisms occur when these surface groups (-OH) react with protons (H+) in electrolyte. The net charge of -OH groups resultant from the reactions responded to the variation of pH in the solution under study. On the silicon oxide surface, the protonation or the de-protonation mechanism of -OH groups occurred. To account the chemical reactions that happened, the surface binding model was used as shown below:

$$SiOH + H_S^+ \overset{K_a}{\Leftrightarrow} SiOH_2^+ \tag{2}$$

$$SiO^- + H_S^+ \underset{K_b}{\Leftrightarrow} SiOH \tag{3}$$

Where $\boldsymbol{H}+$ denotes the proton concentration close to the surface part, Ka and Kb are the equilibrium constants. The surface group protonation/deprotonation affinity is defined as pKa and pKb respectively where the relationship is as shown below:

$$pK_a = -log_{10}K_a, pK_b = -log_{10}K_b \tag{4}$$

Total density of the surface group is given by:

$$N_s = [SiOH] + [SiH_2^+] + [SiO^-] \tag{5}$$

Table I shows the parameters of site-binding model based on different types of oxide used in this work [9][21].

**Table 1** Surface-binding model parameters

| Oxide | pKa | pKb | $N_S(cm^{-2})$ |
|---|---|---|---|
| **SiO2** | -2 | 6 | $5 \times 10^{14}$ |
| **Al2O3** | 6 | 10 | $8 \times 10^{14}$ |
| **Ta2O5** | 2 | 4 | $10 \times 10^{14}$ |

The DGFET transducers in this work are long-channel transistors, hence the current is calculated based on the drift-diffusion formalism. The applied bias is VDS ~ 0.1 V and 0.5 V as smaller VDS is typical for bio sensing applications [9], [15]. The channel length and width were varied based on the long-channel device range as depicted in Figure 2 (b). The figure also displays the variation of top and back oxide thickness with a similar range that was previously studied [9][15]. Table II shows the device geometry and simulation conditions used in this work [20]. The range of pH level used in this work (from pH 3 to 9) was used to get an average response within the range used in most experimental works [9], [13], [22].

**Table 2** Device geometry and simulation conditions

| Parameter | Values range |
|---|---|
| **Sensor width** | 0.1 μm, 1 μm, 10 μm |
| **Sensor length** | 0.25 μm, 1 μm, 10 μm |
| **Front gate oxide thickness** | 2 nm, 4 nm |
| **Back gate oxide thickness** | 50 nm, 100 nm, 150 nm |
| **Silicon body thickness** | 80 nm |
| **Drain voltage** | 0.1 V, 0.5 V |
| **Front gate voltage** | 1V to 5 V |
| **Back gate voltage** | 1V to 5 V |
| **pH level** | 3 to 9 |

## 3. RESULTS AND DISCUSSION

### 3.1 Transfer Characteristics of pH-Ion Sensitive DGFET-based Sensor

Figures 3 (a) and (b) show source-drain current–voltage (I– V) characteristics of DGFETs under study measured for both front and back gate operations, correspondingly. The I–V characteristics demonstrate typical performance which is similar to the metal- oxide-semiconductor FETs (MOSFETs)[15] [23]. The current can be represented by the well-known expression for MOSFETs,

$$I_D = \frac{\varepsilon_i W}{t_i L}\mu V_{DS}^2\left(V_G - V_T - \frac{V_{DS}}{2}\right)(Low\ V_D) \qquad I_D = \frac{\varepsilon_i W}{2t_i L}\mu(V_G - V_T)^2(High\ V_D) \tag{6}$$

Where $\varepsilon_i$ and ti are the dielectric constant and thickness for the dielectric layer respectively, W is the width, while L is the length of the transistor inverted region between source and drain, μ is the mobility of the carrier, and $V_t$ is the threshold voltage. Observed that as the pH value reduces from 9 to 3, the current rises which demonstrates higher conductance of the DGFET for both front and back gate operations respectively. Higher pH values decreased the drain current. For a lower pH solution value, higher density of $H^+$ ions were available in the buffer solution. This will increased the concentration of positive charges on the pH sensing region hence attracting the electrons in the transistor channel subsequently produces higher drain current [24].

The resultant pH sensitivity was taken based on threshold voltage shift which was in agreement with previous studies [9], [12], [24] where the back gate operation can amplify the sensitivity beyond 59mV/pH as depicted in Figure 3 (c). Observed that the threshold voltage shift increased as the pH increased. The front gate operation has sensitivity below the Nernst limit as predicted while the back gate operation amplified the pH detection signal by a factor of 8 as compared to front gate operation. The super-Nernstian characteristics demonstrated by the DGFET was due to the asymmetry factor of front and back oxide capacitances assuming capacitive coupling as experimentally observed in [25], [26][13]. The pH responsivity with capacitive coupling sandwiched between the front/back gates and channels can be explained based on the effect of electrical potential generated thru the pH solution where the front-gate region is capacitively tied to the back gate through the inverted substrate region of the transistor between source and drain [24].

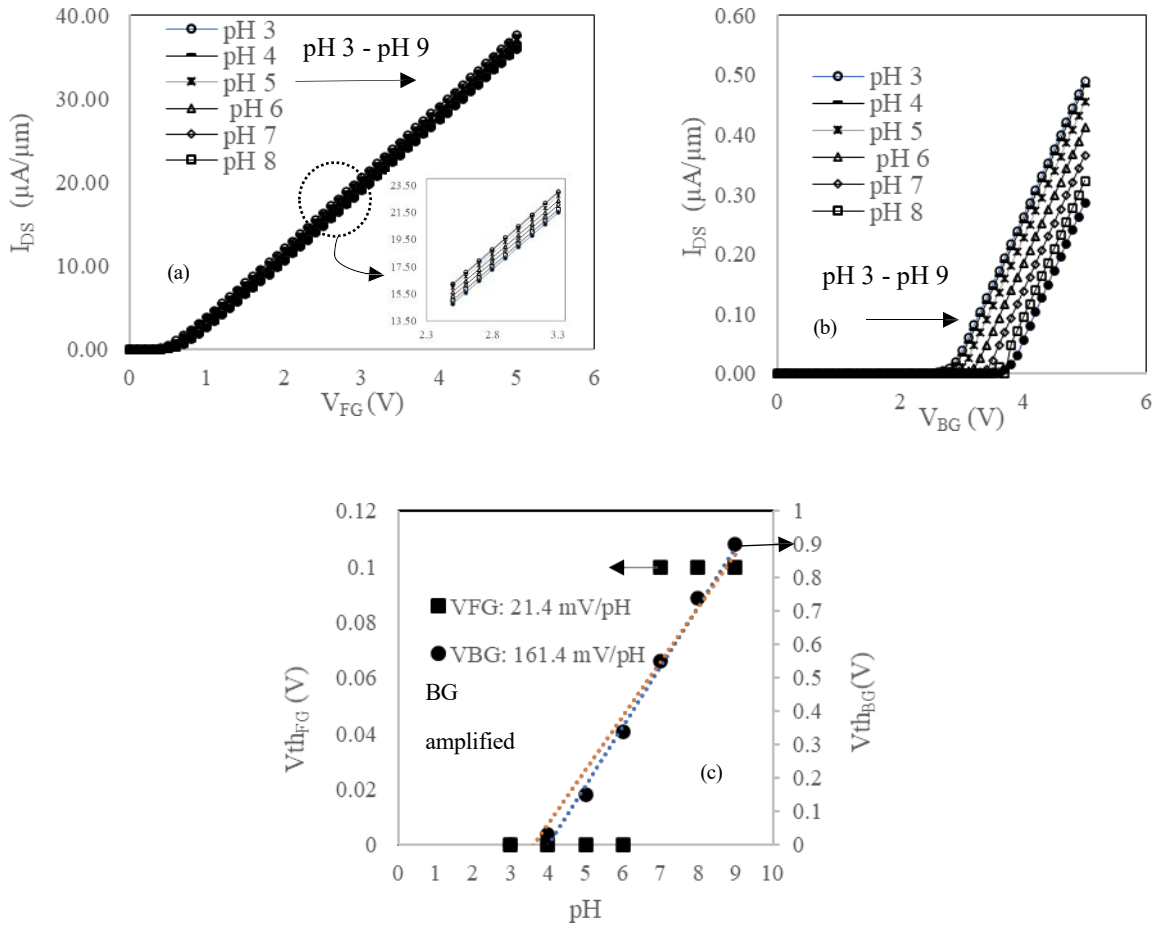


**Figure 3.** (a) IDS-VFG plots with varying pH level (3 - 9) (b) IDS-VBG plots with varying pH levels (3 - 9) (c) Subsequent shifts of Vt shows pH sensitivity below and above the Nernst limit for front and back gate operation respectively.

### 3.2 Effects of Scaling W/L, Top and Bottom Oxide Thickness on Amplification by Back Gate Operation

This section discusses the amplification factor based on a different width and length ratio, (W/L) and the effects of different top and bottom oxide thickness on the transducer performance. Figures 4 (a) and (b) show the transfer characteristics of DGFETs simulated for the front and back gate operations with different lengths for pH 3 and 9 respectively. It is observed that the drain current is higher for shorter DGFET's channel length. By referring to equation 1, the smaller length will contribute to a higher current as shown in both figures.

The DGFET sensors were simulated based on $SiO_2$ as the dielectrics, with drain voltage, VD = 0.5V with varying width and length. The front and back oxide thickness are 4 nm and 150 nm correspondingly.

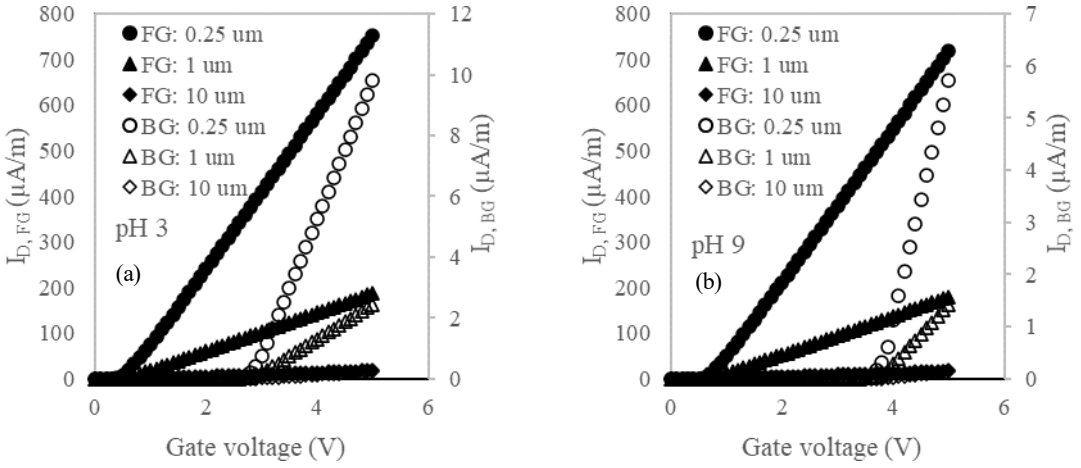


**Figure 4.** IDS-VFG characteristics based on front and back gate operations for different channel length (a) pH 3 (b) pH 9.

Further investigations on the pH responsivity with respect to the different width and length (W/L) ratio are depicted in Table III. Table III shows the sensitivity obtained based on the front and back gate operation and the subsequent amplification percentage and amplification factor by the back gate operation. From the table, it shows that the sensitivity of the DGFET sensors were not width and length dependence for both front and back gate operations. However, the amplification percentage and the amplification factor were similar if W/L gives similar ratio regardless of the value of W and L. Another interesting fact is that for W = 10 μm, smaller length leads to lowest sensitivity for the back gate operation. This is due to the area of the pH-sensitive surface reducing as the length of channel reduces hence the number of measurable $H^+$ ions in the aqueous reduces. Referring to equation (6), the current ID increases with decreasing l, hence decrease in the resistance of the current channel with constant voltage $V_D$. The pH sensitivity decreases when the channel length reduces as the resistance of the channel Rch decreases. Owing to the resistance of the channel $R_{ch}$ decreases, its modulation is hindered under the result of the H+ ions [23].

Similar to previously reported, all range of the W/L DGFETs simulated gave sensitivity below 59mV/pH for front gate operations and above the 59mV/pH for back gate operations [24]. The range of W and L are based on simulation values that can be simulated using the Nanohub.

**Table 3** Sensitivity, amplification percentage and factor based on scaled DGFETs

| W/L | W/L | Front gate operation (mV/pH) | Back gate operation (mV/pH) | Amplification percentage (%) | Amplification factor |
|---|---|---|---|---|---|
| **1/0.25** | 4 | 14.3 | 171.4 | 91.66 | 12.0 |
| **1/1** | 1 | 32.1 | 178.6 | 82.03 | 5.6 |
| **1/10** | 0.1 | 32.1 | 160.7 | 80.02 | 5.0 |
| **0.1/0.25** | 0.4 | 35.7 | 167.9 | 78.74 | 4.7 |
| **0.1/1** | 0.1 | 32.1 | 160.7 | 80.02 | 5.0 |
| **0.1/10** | 0.01 | NA | NA | NA | NA |
| **10/10** | 1 | 32.1 | 178.6 | 82.03 | 5.6 |
| **10/1** | 10 | NA | 164.3 | NA | NA |
| **10/0.25** | 40 | NA | 21.4 | NA | NA |

To investigate the sensitivity based on different thickness of top and bottom oxide of the DGFETs, the transistor with W/L = 0.1/0.25 with different top oxide thicknesses were used, 2 nm and 4 nm with varying bottom oxide thicknesses. The corresponding sensitivity graphs are shown in Figures 5 (a) – (d) based on front and bottom gate operations respectively. Similar to previous results, all front gate operations had sensitivity below the Nernst limit while all back-gate operations had sensitivity beyond the Nernst limit. Both top oxide thickness, 2 nm and 4 nm are smaller than the back oxide thickness which exhibited the asymmetry design feature hence able to contribute to the pH responsivity beyond the Nernst limit [15][24]. Remarkable observation indicates that as the bottom oxide thickness is increased, the pH responsivity significantly increased [11], [15], [24]. The improved pH responsivity based on the increase of the bottom oxide thickness can be explained based on the capacitive coupling ratio $C_{FG}/C_{BG}$ effect. This effect is depends on the biasing condition and geometry of the DGFET as the transducer [24]. Only the back oxide scale improved the sensitivity while the top oxide scale does not exhibit any improvement trend. In [9], the increasing of back gate oxide thickness improved sensitivity, but increasing front gate oxide thickness reduced the sensitivity.

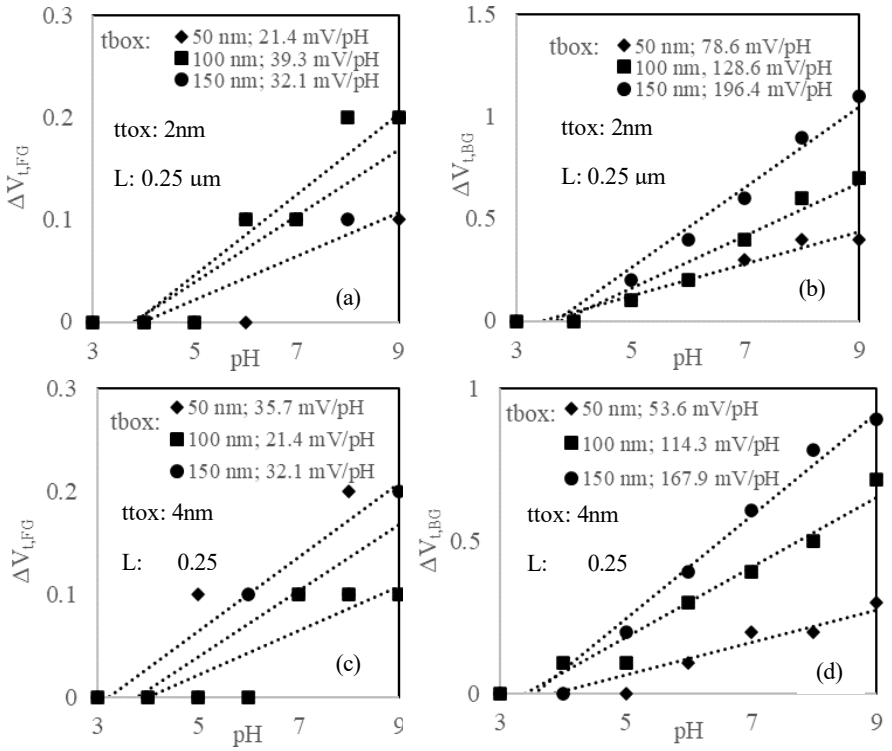


**Figure 5.** Shift of threshold voltage with varying bottom oxide thicknesses with top oxide thickness, 2 nm in (a) front gate operation and (b) back gate operation. Shift of threshold voltage with varying bottom oxide thicknesses with top oxide thickness, 4 nm in (c) front gate operation (d) back gate operation.

### 3.3 Effects of Different Oxide Dielectrics on Sensitivity

To investigate the pH responsivity based on different types of top oxide, three types of oxides consist of $SiO_2$, $Al_2O_3$ and $Ta_2O_5$ were used in this work as shown in Figures 6 (a), (b) and (c) respectively. $Al_2O_3$ and $Ta_2O_5$ gate oxide exhibited better pH responsivity as compared to $SiO_2$. Similarly observed in[15][27], $Al_2O_3$ was better than $SiO_2$ but still limited by the Nernst limit for the single gate FET based sensor. The improved pH responsivity was also reported to be better for $Al_2O_3$ than $SiO_2$ owing to the higher buffer capacity of the $Al_2O_3$ surface [28][22]. In [22], high-k gate dielectric such as $Al_2O_3$ was shown to be better than $SiO_2$ and thicker gate dielectric can be employed by maintaining the sensitivity hence lessens the leakage current which significantly become robust in fluid. $Al_2O_3$ offers sensitivity enhancement based on the increased dielectric

constant that increased the capacitance hence the sensitivity. On the other hand, high sensitivity measurement was achieved as the effect of capacitance on the subthreshold swing value is reduced when the CMOS-compatible ISFET with $Ta_2O_5$ sensitive surface is adopted in the subthreshold working mode [29]. In [30], the $Ta_2O_5$can be used as the high dielectric constant, proton conductor and catalyst. The $Ta_2O_5$ based pH sensors exhibited high sensitivity, small drift effect and good surface quality. According to [31], the ratio of Ta/O at the surface is a critical value for sensitivity detection of pH. It is suggested that, at the surface region the increase of O-sites can improve the sensitivity of the detecting membrane. Surface hydrolysis of $Ta_2O_5$ when immersed in solution form the tantalum hydroxyl groups (Ta-OH). It became charged when reacting to solutions comprising H+/OH- ions by contributing or getting protons [31].

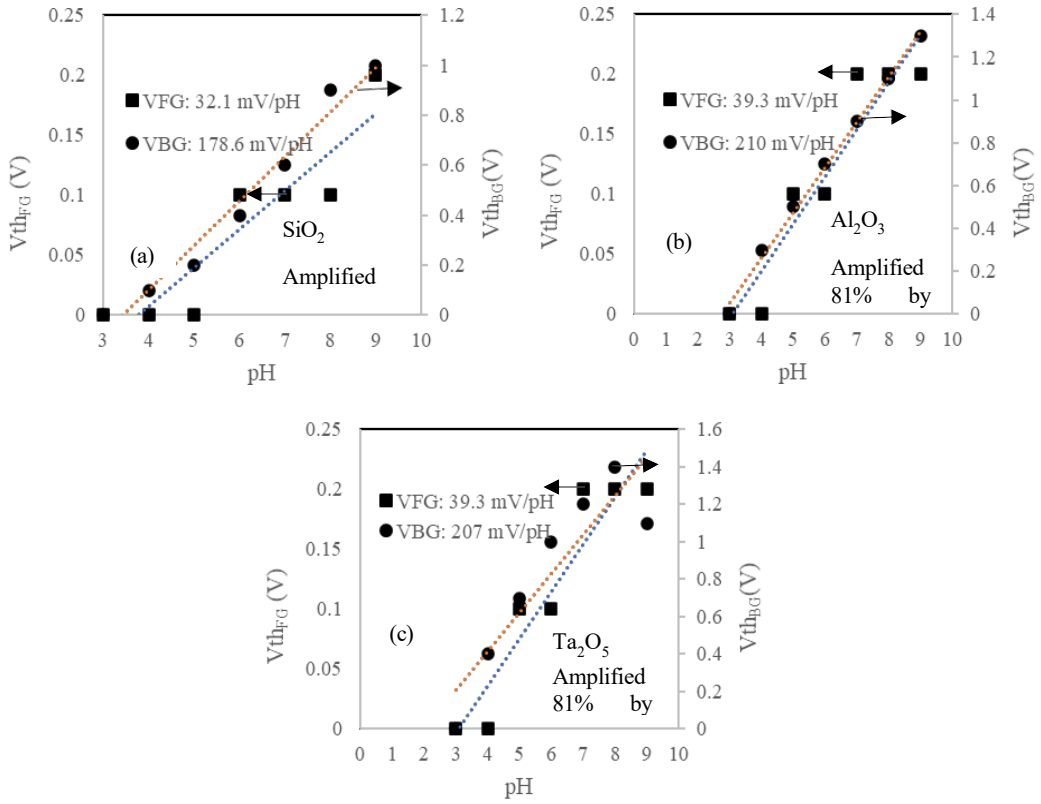


**Figure 6.** Shift of threshold voltage based on front and back gate operation using different top- oxide-electrolyte interfaces (a) $SiO_2$ (b) $Al_2O_3$ (c) $Ta_2O_5$

## 4. CONCLUSION

In this study, improved pH sensitivity which was higher than 59mV/pH (Nernst limit) was demonstrated through back-gate operation of DGFETs. The amplification was exhibited due to the capacitive coupling effects owing to the asymmetric thickness of front/back oxide. Thicker back oxide contributed to high sensitivity while similar W/L ratio exhibited the same responsivity level. The use of high-k dielectrics, for instance $Al_2O_3$ and $Ta_2O_5$ can further increase the sensitivity response. Hence, DGFET-based sensor is an accomplished label-free transducer for detection of various biological events which can be further optimized through the geometrical configurations and the type of dielectrics used.

**ACKNOWLEDGEMENTS**

We acknowledge support from the Center of Printable Electronics, Research Management Center, University of Malaya and School of Electrical Engineering, College of Engineering, Universiti Teknologi MARA, Shah Alam. The authors acknowledge the funding from the Ministry of Education (MOE) under Fundamental Research Grant Scheme (FRGS: FRGS/1/2019/TK04/UITM/02/20).

**REFERENCES**

[1] C. M. Lim, I. K. Lee, K. J. Lee, Y. K. Oh, Y. B. Shin, & W. J. Cho, Sci. Technol. Adv. Mater., vol. 18, no. 1, (2017) pp. 17–25.
[2] Y.-C. Syu, W.-E. Hsu, & C.-T. Lin, ECS J. Solid State Sci. Technol., vol. 7, no. 7, (2018) pp. Q3196–Q3207.
[3] H. Li, X. Liu, L. Li, X. Mu, R. Genov, & A. J. Mason, Sensors (Switzerland), vol. 17, no. 1, (2017).
[4] H. J. Jang & W. J. Cho, Sci. Rep., vol. 4, (2014) pp. 1–8.
[5] M. Kaisti, Biosens. Bioelectron., vol. 98, no. June, (2017) pp. 437–448.
[6] S. B. Hashim, A. B. Rosli, Z. Zulkifli, W. Fazlida, H. Abdullah, & S. H. Herman, Sci. Lett., vol. 16, no. 2, (2022) pp. 73–83.
[7] S. Bakhtiar Hashim, Z. Zulkiii, S. Hana Herman, & Z. Zulkifli, Research Square, (2021).
[8] S. Sanjay, M. Hossain, A. Rao, & N. Bhat, npj 2D Mater. Appl., vol. 5, no. 1, (2021).
[9] A. Shadman, E. Rahman, & Q. D. M. Khosru, Sens. Bio-Sensing Res., vol. 11, (2016) pp. 45–51.
[10] E. Rahman, A. Shadman, & Q. D. M. Khosru, Sens. Bio-Sensing Res., vol. 13, (2017) pp. 49–54.
[11] J. Go, P. R. Nair, & M. A. Alam, J. Appl. Phys., vol. 112, no. 3, (2012) pp. 1–10.
[12] J. H. Ahn *et al*., Appl. Phys. Lett., vol. 102, no. 8, (2013).
[13] R. Pfattner *et al*., Adv. Electron. Mater., vol. 5, no. 1, (2019) pp. 1–9.
[14] P. Dwivedi, R. Singh, & Y. S. Chauhan, IEEE Sens. J., vol. 21, no. 3, (2021) pp. 3233–3240.
[15] J. Go, P. R. Nair, B. Reddy, B. Dorvel, R. Bashir, & M. A. Alam, Tech. Dig. - Int. Electron Devices Meet. IEDM, vol. 2, (2010) pp. 202–205.
[16] K. Sun *et al*., Nanotechnology, vol. 27, no. 28, (2016).
[17] X. Chen, C. Liu, & S. Mao, Nano-Micro Lett., vol. 12, no. 1, (2020) pp. 1–24.
[18] Y. J. Huang *et al*., Tech. Dig. - Int. Electron Devices Meet. IEDM, vol. 2016-Febru, (2015) pp. 29.2.1-29.2.4.
[19] J. H. Jeon & W. J. Cho, Sci. Technol. Adv. Mater., vol. 21, no. 1, (2020) pp. 371–378.
[20] N. Pradeep Ramachandran *et al*., nanoHUB, Purdue University, (2014).
[21] D. Landheer, G. Aers, W. R. McKinnon, M. J. Deen, & J. C. Ranuarez, J. Appl. Phys., vol. 98, no. 4, (2005).
[22] B. Reddy *et al*., Biomed. Microdevices, vol. 13, no. 2, (2011) pp. 335–344.
[23] F. Gasparyan, I. Zadorozhnyi, H. Khondkaryan, A. Arakelyan, & S. Vitusevich, Nanoscale Res. Lett., vol. 13, (2018).
[24] J. H. Ahn, B. Choi, & S. J. Choi, J. Appl. Phys., vol. 128, no. 18, (2020).
[25] C. M. Lim, I. K. Lee, K. J. Lee, Y. K. Oh, Y. B. Shin, & W. J. Cho, Sci. Technol. Adv. Mater., vol. 18, no. 1, (2017) pp. 17–25.
[26] T. Wu, A. Alharbi, K. D. You, K. Kisslinger, E. A. Stach, & D. Shahrjerdi, ACS Nano, vol. 11, no. 7, (2017) pp. 7142–7147.
[27] A. Hasan & N. A. Sultana, "Performance Analysis of Nano-scale Double-Gated Field Effect Transistor pH Sensor," in Proc. International Conference on Mechanical Engineering and Applied Science, (2017).
[28] O. Knopfmacher *et al*., Nano Lett., vol. 10, no. 6, (2010) pp. 2268–2274.
[29] Y. Wang, M. Yang, & C. Wu, Sensors (Switzerland), vol. 20, no. 23, (2020) pp. 1–16.

[30] L. Manjakkal, D. Szwagierczak, & R. Dahiya, Prog. Mater. Sci., vol. 109, no. December 2019, (2020) pp. 100635.
[31] D. H. Kwona, B. W. Cho, C. S. Kim, & B. K. Sohn, Sensors Actuators, B Chem., vol. 34, no. 1–3, (1996) pp. 441–445.